Partial Differential Equations in Applied Mathematics 14 (2025) 101214

Contents lists available at ScienceDirect

Partial Differential Equations in Applied Mathematics

journal homepage: www.elsevier.com/locate/padiff

Dark lump collision phenomena to a nonlinear evolution model in harmonic crystals

Muhammad Abubakar Isah [a,*], Asif Yokus [b], Ibrahim Isah [c]

[a] Department of Mathematics, Istanbul Commerce University, 34445, Istanbul, Turkey
[b] Firat University, Faculty of Sciences, Department of Mathematics, Elazig, Turkey
[c] Department of Art and Humanities School of General and Remedial Studies, Kano State Polytechnic, Nigeria

ARTICLE INFO

Keywords:
The new kdV equation
Two-wave solutions
Hirota bilinear method
Lump waves
Lump-periodic waves

ABSTRACT

In this paper, we examine the innovative KdV model, which has a profound impact on our understanding of a range of nonlinear occurrences of ion-acoustic waves in plasma and acoustic waves in harmonic crystals. Using the appropriate transformations, Hirota bilinearization is performed to generate the solutions. Using trigonometric, hyperbolic, and exponential functions, we generate collision aspects between lumps and other solutions in order to establish some more interaction solutions with some innovative physical characteristics. We obtain the two-wave, dark lump wave and lump-periodic solutions. The identified solutions are visually represented. In the fields of shallow-water waves, ion-acoustic waves in plasma, and acoustic waves in harmonic crystals, the current work is extensively exploited to describe a variety of remarkable physical events. To ensure the accuracy of the result, all the obtained solutions are placed in the model.

1. Introduction

The fact that waves occur constantly in a variety of shapes is a basic feature of the universe in which we live. Electric impulses traveling through semiconductors or conductive materials, human-to-human voice transmission, and water movements on ocean surfaces are only a few of the processes in which they enable the transfer of energy. Energy transmission across various systems is greatly aided by such wave occurrences. It is essential to know how waves move, interact, and react to their surroundings. In addition to providing a strong mathematical foundation for modeling and characterizing these intricate wave dynamics, nonlinear partial differential equations (PDEs) also provide light on the underlying processes and wider implications of these dynamics for science and industry.[1] Initial uses of partial differential equations were in the study of surfaces[2,3] in geometry,[4–6] as well as a variety of mechanical problems. In the 1800s, leading mathematicians from all over the world showed a strong interest in studying the complex structure of partial differential equations (PDEs). Comprehending these equations is essential for interpreting a variety of natural phenomena, leading to mathematical investigation and notable breakthroughs in disciplines such as fluid dynamics, engineering, and physics. Breakthrough findings in the study of PDEs have influenced contemporary mathematical ideas and addressed pressing problems. Modern applied mathematics and nonlinear dynamics studies were founded during this era of development as mathematicians delved deeply into the complex connections and behaviors that PDEs represented.[7]

Optical solitons are specific solutions to nonlinear partial differential equations (NLPDEs)[8] that are of great interest to the physical and natural sciences. There has been much interest in the stability of these self-reinforcing wave transmissions and their relevance to phenomena such as wave propagation and fiber optics. Scholars have employed a wide range of approaches, such as; the deep neural network model and the bilinear technique are combined in the bilinear neural network (BNN) approach,[9] which enables the discovery of further unidentified and fascinating NLPDE solutions as well as the flexible production of a variety of test functions, other methods include; the homoclinic technique,[10] the cosine function technique,[11] the Bernoulli sub-equation function technique,[12,13] the $(1/G')$−expansion technique,[14] the bilinear neural network method,[15,16] the Lie group symmetry method,[17] the sub equation method,[18] bilinear residual network method[19] the improved F-expansion technique,[20] the generalized exponential rational function technique,[21,22] Sardar-sub equation technique,[23] the auto-Bäcklund transformation technique,[24] extended rational sine–cosine technique,[25] improved modified extended tanh-function approach,[26] modified auxiliary equation technique,[27] the φ^6-model expansion technique[28–33] and so on to get different soliton

* Corresponding author.
E-mail addresses: maisah@ticaret.edu.tr (M.A. Isah), asfyokus@yahoo.com (A. Yokus), ibistatistics@kanopoly.edu.ng (I. Isah).

https://doi.org/10.1016/j.padiff.2025.101214
Received 8 January 2025; Received in revised form 20 April 2025; Accepted 24 April 2025
Available online 9 June 2025
2666-8181/© 2025 The Author(s). Published by Elsevier B.V. This is an open access article under the CC BY-NC-ND license (http://creativecommons.org/licenses/by-nc-nd/4.0/).

solutions. The unique contributions of each technique to the understanding and use of solitons push the theoretical and practical limits of nonlinear study.

Lump waves are regarded as a non-linear wave phenomenon that may be observed in several disciplines. Theoretically, lump waves are considered as the limit form because of their tremendous propagation energy. The lump would therefore be harsh and horrible for some systems, including the ocean and finance. Therefore, research on lump waves helps to develop a better understanding and predict possible extremes for nonlinear partial differential equations.[34,35] Among the most significant findings for nonlinear PDEs are lump solutions.[36,37] Numerous non-integrable equations have lump solutions. Furthermore, several studies have demonstrated the existence of collision characteristics between lumps and other types of nonlinear equation solutions.[38,39]

Recently, Arif[40] considered a new (2+1)-dimensional KDV model to study multi-soliton solutions and their dynamical collisions, which found an induce collisions between these kind of waves and their multi-soliton solutions. In this current article, as we believed, no study has applied this model with the methodology described. This model will solve by providing lump-wave, lump- periodic, and two-wave solitons. We are unaware of any prior research that has been done to evaluate the model with the proposed techniques. The behavior of the PDEs is still unknown, and more of these solutions needs to be investigated.

The following sections serve as the foundation for the major steps on which this study is developed. The Hirota bilinear approach definition is given in Section 2. Section 3 describes how to create the bilinear transformation of the new KdV model. In Section 4, the appropriate transformation via the Hirota bilinear equation is employed to generate lump waves to the new KdV model. The corresponding two-dimensional, 3-dimensional, and contour plots also effectively display the structural properties of the derived solitary wave solutions. In Section 5, the interaction between the lump-periodic wave solution will be examined, their corresponding graphs will be shown, while in Section 6, we will study two-wave solutions for the given model. In Section 7, the physical phenomena of the analytical solutions are studied, and Concluding remarks are made in Section 8.

2. Hirota bilinearization

A model referred to as the direct approach is highly regarded due to its effectiveness in constructing N-solitons solutions for fully integrable models.[41,42] Hirota introduced the technique. Also, Griffiths[43] offers illustrations for some of the application possibilities that utilize the method. Hirota employed the following method below to apply a bilinear differential operator to a pair of functions(g, h), dependent on a real variable x[10]:

$$D_x(g.h) = \left(\partial_x - \partial_{x'}\right) g(x)h(x')\,|_{x'=x}\,. \tag{2.1}$$

To understand the D-operator more clearly, consider the following concise results below.

$$D_x(g.h) = g_x h - g h_x = -D_x(h.g), \tag{2.2}$$

$$D_x^2(g.h) = g_{xx}h - 2g_x h_x + g h_{xx}, \tag{2.3}$$

$$D_x D_t(g.h) = g_{xt}h - g_t h_x - g_x h_t + g h_{xt}. \tag{2.4}$$

In a situation when $g = h$

$$D_x^{2n-1} g.g = 0, \tag{2.5}$$

$$D_x^{2n} g.g = \sum_{k=0}^{2n} (-1)^{2n-k} \binom{2n}{k} \left(\partial_x^k g\right)\left(\partial_x^{2n-k} g\right). \tag{2.6}$$

Similarly, the bilinear partial derivative expression is equal to

$$D_x^n D_t^m(g.g) = \sum_{i=0}^{n}\sum_{j=0}^{m} (-1)^{m+n-(j+i)} \binom{n}{i}\binom{m}{j}\left(\partial_x^i \partial_t^j g\right)\left(\partial_x^{n-i}\partial_t^{m-j} g\right), \tag{2.7}$$

for $n, m \geq 1$.

3. The new-KdV equation expressed in its bilinear form

In this section, we solve the new KdV model applying Hirota's bilinear approach and obtain new solitary wave solutions. The equation is presented as follows.

$$Q_t + \alpha Q_x Q_y + Q_{xxy} = 0, \tag{3.1}$$

In this context, $Q(x, y, t)$ is defined as the surface profile, and α denotes the nonlinear convection coefficient. The wave time-dependent propagation term is indicated by Q_t while, the waves spreading and steepening effects within the model is described by Q_{xxy} and $Q_x Q_y$. The new KdV equation has proven useful in explaining various physical phenomena in great detail, including acoustic waves in harmonic crystals and ion-acoustic waves in plasma.[40]

Some works related to the model (3.1) have been done, among them are; Chuan-Jian, et al.[44] used the extended homoclinic test function approach to derive soliton solutions such kinky periodic solitary-wave solutions, periodic soliton solutions, and cross kink-wave solutions for the new (2+ 1)-dimensional KdV equation. Lie point symmetries associated with the model are investigated, Painlevé analysis for this equation is also presented and the soliton solution is obtained directly from the Bäcklund transformation by Shen[45]. By employing a proper algebraic transformation and the Riccati equation Yu-Feng et al.[46] obtained soliton solutions via regarding the variable in the Riccati equation as the independent variable then extend the (2+ 1)-dimensional KdV equation into (3+ 1)-dimensional equation to derive the two-soliton solutions. By comparing our results to the ones existing in the literature our solutions are new.

We utilize the bilinear transformation method, to derive new solitary wave solutions for the KdV equation. Which happened to be a robust symbolic computation technique for generating multiple soliton solution to the model (3.1).

Setting up the transformation

$$Q(x, y, t) = \frac{6}{\alpha}(\ln g)_x, \tag{3.2}$$

The below bilinear form can be used to represent the new KdV model,

$$g g_{xt} - g_x g_t + g g_{xxxy} - g_y g_{xxx} + 3 g_{xx} g_{xy} - 3 g_x g_{xxy} = 0. \tag{3.3}$$

where $g = g(t, x, y)$ is a function of t, y and x.

4. The new KdV model with its associated lump solutions

Let us consider the function g to have a particular structure, to determine the exact lump solutions we utilize the Hirota's bilinear form[34,35]

$$g(x, y, t) = \lambda^2 + \mu^2 + n, \tag{4.1}$$

where

$$\mu = m_3 t + m_1 x + m_2 y + m_4,\ \lambda = m_7 t + m_5 x + m_6 y + m_8, \tag{4.2}$$

where m_2, m_6 are the wave numbers, m_1, m_5 are the frequencies, m_3, m_7 are the velocities and m_3, m_8 are constants.[10] The following equations are obtained when the above relations are used.

$$\begin{aligned}
-2m_1 m_3^3 - 2m_5 m_7 m_3^2 - 2m_1 m_7^2 m_3 - 2m_5 m_7^3 &= 0,\\
-2m_1 m_3 m_2^2 + 2m_5 m_7 m_2^2 - 4m_3 m_5 m_6 m_2 - 4m_1 m_6 m_7 m_2 + 2m_1 m_3 m_6^2 - 2m_5 m_6^2 m_7 &= 0,\\
-2m_3 m_1^3 - 2m_5 m_7 m_1^2 - 2m_3 m_5^2 m_1 - 2m_5^3 m_7 &= 0,\\
-4m_1 m_2 m_3^2 - 4m_5 m_6 m_3^2 - 4m_1 m_2 m_7^2 - 4m_5 m_6 m_7^2 &= 0,\\
-4m_1^2 m_3^2 - 4m_5^2 m_3^2 - 4m_1^2 m_7^2 - 4m_5^2 m_7^2 &= 0,\\
-4m_2 m_3 m_1^2 - 4m_6 m_7 m_1^2 - 4m_2 m_3 m_5^2 - 4m_5^2 m_6 m_7 &= 0,\\
-4m_1 m_4 m_3^2 - 4m_5 m_8 m_3^2 - 4m_1 m_4 m_7^2 - 4m_5 m_7^2 m_8 &= 0,
\end{aligned} \tag{4.3}$$

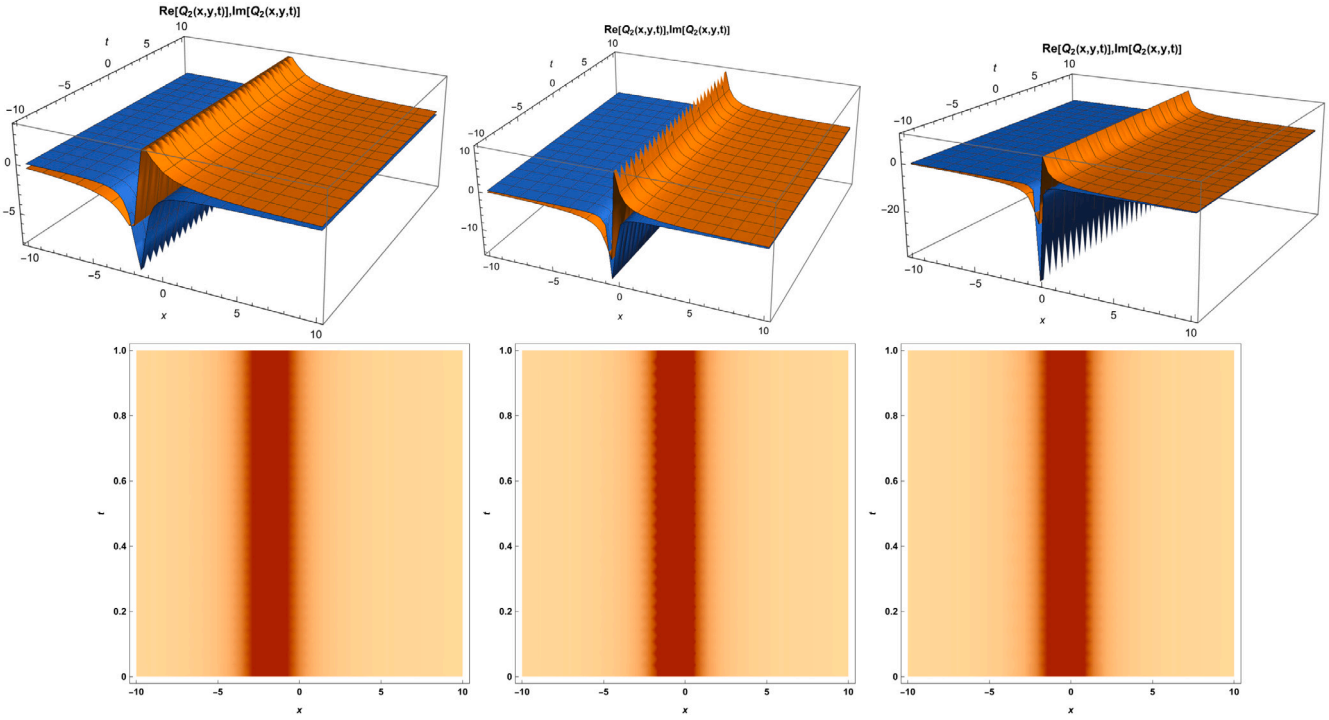


Fig. 1. The 3D and density plots of Eq. (4.5) for $\alpha = 1.5, m_2 = 0.3, m_3 = m_4 = m_6 = 0.2, m_8 = 1.6, n = 0.2$ at $m_5 = 0.5, m_5 = 1.5$ and $m_5 = 2.8$ respectively.

$$
\begin{aligned}
&-4m_1m_2m_3m_4 - 4m_3m_4m_5m_6 + 4m_2m_4m_5m_7 - 4m_1m_4m_6m_7\\
&-4m_2m_3m_5m_8 + 4m_1m_3m_6m_8 - 4m_1m_2m_7m_8 - 4m_5m_6m_7m8 = 0,\\
&-4m_3m_4m_1^2 - 4m_7m_8m_1^2 - 4m_3m_4m_5^2 - 4m_5^2m_7m_8 = 0,\\
&2m_3m_1n + 2m_5m_7n + 12m_2m_1^3 + 12m_5m_6m_1^2 - 2m_3m_4^2m_1 + 12m_2m_5^2m_1 + 2m_3m_8^2m_1\\
&-4m_4m_7m_8m_1 - 2m_5m_7m_8^2 + 12m_5^3m_6 + 2m_4^2m_5m_7 - 4m_3m_4m_5m_8 = 0.
\end{aligned}
$$

We obtain the solution of Eq. (4.3) using a mathematical package, along with Eqs. (4.1), (3.3) and (4.2) the solution sets are found as;

Set I:

$$m_1 = -im_5,\ m_7 = -im_3,\ n = 0. \tag{4.4}$$

These values generate the lump solutions

$$Q_2(x,y,t) = \frac{6\left(2m_5\left(-im_3t + m_5x + m_6y + m_8\right) - 2im_5\left(m_3t - im_5x + m_2y + m_4\right)\right)}{\alpha\left(\left(m_3t - im_5x + m_2y + m_4\right)^2 + \left(-im_3t + m_5x + m_6y + m_8\right)^2\right)}. \tag{4.5}$$

Lump solutions are of great interest in fields like fluid dynamics, quantum mechanics, and optics due to their localization property. They decay in all spatial directions and represent a stable, localized structure that can travel without changing its shape, which is typically found in nonlinear wave equations.

Fig. 1 displays a smooth surface of Eq. (4.5) with a distinct crest and trough, little oscillation, and an average wave height. The lump solution behaves less oscillatorily and more steadily at lower frequency $m_5 = 0.5$, indicating confined energy and an unaltered wave structure. There is less localized energy and a more complicated wave structure in the lump solution at medium frequency $m_5 = 1.5$, as evidenced by the increased oscillations. The lump solution exhibits steep troughs and extreme oscillations at higher frequency $m_5 = 2.8$, suggesting a greater vulnerability to instability and dispersion and less confined energy.

Fig. 2 depicts a smooth surface of Eq. (4.5) with noticeable crests and troughs, minimal oscillation, and average wave height. At lower frequencies, the lump solution exhibits less oscillatory behavior, suggesting contained energy and unchanged wave shape. It has a more complex wave structure and less localized energy at mid-frequencies. It exhibits severe oscillations and steep peaks at higher frequencies, suggesting increased instability and dispersion.

5. Lump-periodic solutions

The combination of lump and periodic solutions that have localized structures and behave periodically over space or time is called lump-periodic solutions. It has many applications in fluid dynamics, quantum mechanics, and optics due to its complex wave structure stability. The following relationship is used to retrieve the lump periodic wave solutions[36]:

$$g(x,y,t) = n_2\cos\left(\mu_2\right) + n_1\cosh\left(\mu_1\right) + n_3\cosh\left(\mu_3\right), \tag{5.1}$$

where

$$
\begin{aligned}
\mu_3 &= l_3t + l_1x + l_2y,\\
\mu_2 &= m_3t + m_1x + m_2y,\\
\mu_1 &= r_3t + r_1x + r_2y.
\end{aligned} \tag{5.2}
$$

where $l_i, m_i, r_i\ (i = 1,2,3)$ are constants, below system of equations is found by replacing Eqs. (5.1), (5.2) into Eq. (3.3) and then collecting the coefficients:

$$
\begin{aligned}
&-3m_1^2n_1n_2r_1r_2 - 3m_2m_1n_1n_2r_1^2 + m_2m_1^3n_1n_2 - m_3m_1n_1n_2 + n_1n_2r_1^3r_2 + n_1n_2r_1r_3 = 0,\\
&4m_1^3m_2n_2^2 - m_1m_3n_2^2 = 0,\\
&3l_1^2n_1n_3r_1r_2 + 3l_2l_1n_1n_3r_1^2 + l_2l_1^3n_1n_3 + l_3l_1n_1n_3 + n_1n_3r_1^3r_2 + n_1n_3r_1r_3 = 0,\\
&-3l_1^2m_1m_2n_2n_3 - 3l_2l_1m_1^2n_2n_3 + l_2l_1^3n_2n_3 + l_3l_1n_2n_3 + m_1^3m_2n_2n_3 - m_1m_3n_2n_3 = 0,\\
&l_1^3m_2n_2n_3 + 3l_2l_1^2m_1n_2n_3 - 3l_1m_1^2m_2n_2n_3 + l_1m_3n_2n_3 - l_2m_1^3n_2n_3 + l_3m_1n_2n_3 = 0,\\
&4l_2l_1^3n_3^2 + l_3l_1n_3^2 = 0,\\
&m_1^3\left(-n_1\right)n_2r_2 - 3m_2m_1^2n_1n_2r_1 + 3m_1n_1n_2r_1^2r_2 + m_1n_1n_2r_3 + m_2n_1n_2r_1^3 + m_3n_1n_2r_1 = 0,\\
&l_1^3\left(-n_1\right)n_3r_2 - 3l_2l_1^2n_1n_3r_1 - 3l_1n_1n_3r_1^2r_2 - l_1n_1n_3r_3 - l_2n_1n_3r_1^3 - l_3n_1n_3r_1 = 0,\\
&4n_1^2r_2r_1^3 + n_1^2r_3r_1 = 0.
\end{aligned} \tag{5.3}
$$

The following results are obtained by solving Eq. (5.3).

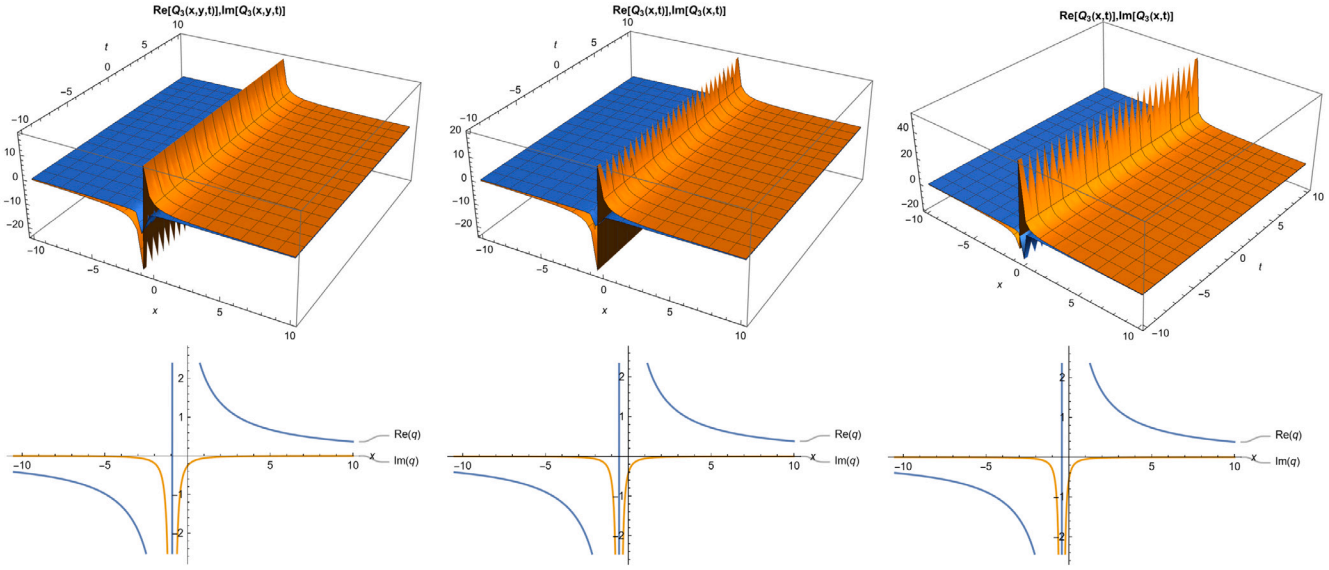


Fig. 2. The three-dimensional and two-dimensional graphs of Eq. (4.5) for $\alpha = 1.5, m_2 = 0.3, m_3 = 2.2, m_4 = m_6 = 0.2, m_8 = 8.1, n = 0.2$ at $m_5 = 4.5, m_5 = 7.5$ and $m_5 = 9.8$ respectively.

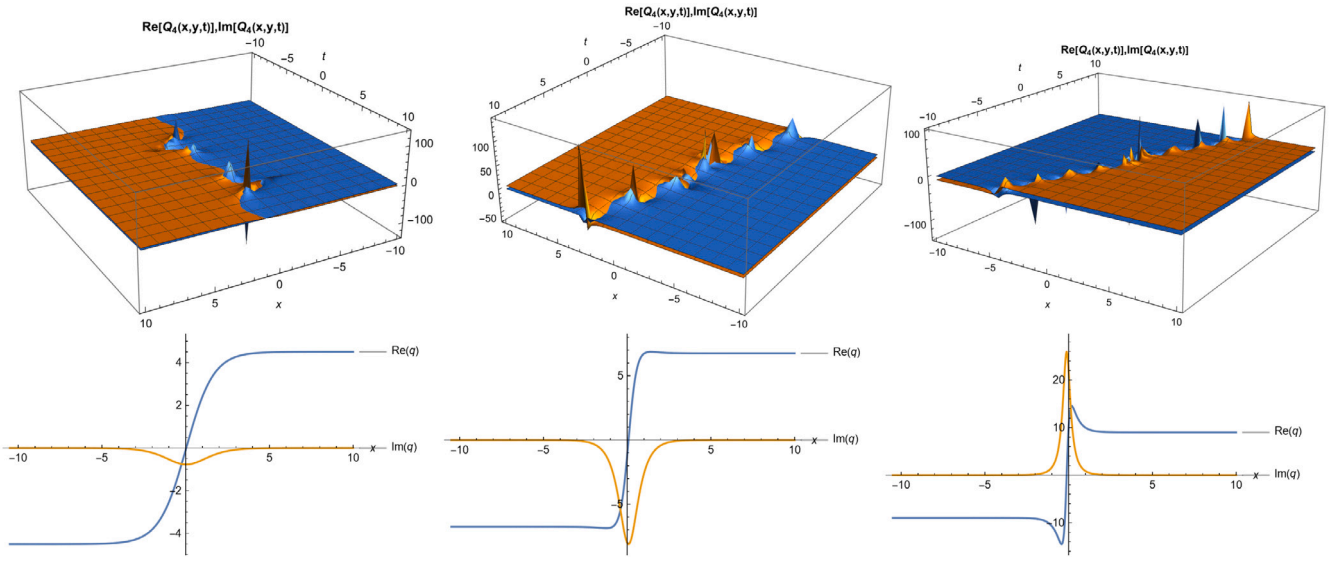


Fig. 3. The three-dimensional and two-dimensional plots of Eq. (5.5) for $\alpha = 0.8, l_2 = 0.2, m_2 = 0.5, n_1 = 1.6, n_2 = 1.7, n_3 = 0.5$ at $l_1 = 0.6, l_1 = 0.9$ and $l_1 = 1.2$ respectively.

Set I:

$$m_1 = -il_1,\ m_3 = -4l_1^2 m_2,\ l_3 = -4l_1^2 l_2,\ n_1 = 0. \tag{5.4}$$

By using the Eqs. (3.2), (5.1), (5.2) and (5.4), the following result is obtained

$$Q_4(x,y,t) = \frac{6l_1\left(n_3\sinh\left(l_2\left(y-4l_1^2t\right)+l_1x\right)+n_2\sinh\left(l_1x+im_2\left(y-4l_1^2t\right)\right)\right)}{\alpha\left(n_3\cosh\left(l_2\left(y-4l_1^2t\right)+l_1x\right)+n_2\cosh\left(l_1x+im_2\left(y-4l_1^2t\right)\right)\right)}. \tag{5.5}$$

The lump-periodic solution of Eq. (5.5) shows in Fig. 3 has an equilibrium periodic shape and stable, less oscillating movements at lower frequency $l_1 = 0.6$. A uniform wave structure with mild periodic modulation and well-localized energy is indicated by this. The $3D$ and $2D$ graphs exhibit lump-periodic behavior, displaying a periodic structure with mild peaks and valleys. The imaginary section (orange curve) shows a slight change close to $x = 0$, but the real component (blue curve) shifts smoothly. As the frequency parameter increases from $l_1 = 0.9$ to $l_1 = 1.2$, lump-periodic solutions exhibit faster and more pronounced fluctuations. Both $2D$ and $3D$ charts exhibit sharper transitions and more pronounced peaks and troughs that come with higher frequencies. These findings will be crucial for applications that need the coherence and stability of wave structures with periodic behavior.

Set II:

$$m_3 = 4m_1^2 m_2,\ n_1 = 0,\ n_3 = 0, \tag{5.6}$$

we get

$$Q_5(x,y,t) = -\frac{6m_1\tan\left(m_2\left(4m_1^2t+y\right)+m_1x\right)}{\alpha}. \tag{5.7}$$

Set III:

$$r_1 = im_1,\ r_3 = 4m_1^2 r_2,\ l_1 = -im_1,\ l_3 = 4l_2 m_1^2,\ m_3 = 4m_1^2 m_2, \tag{5.8}$$

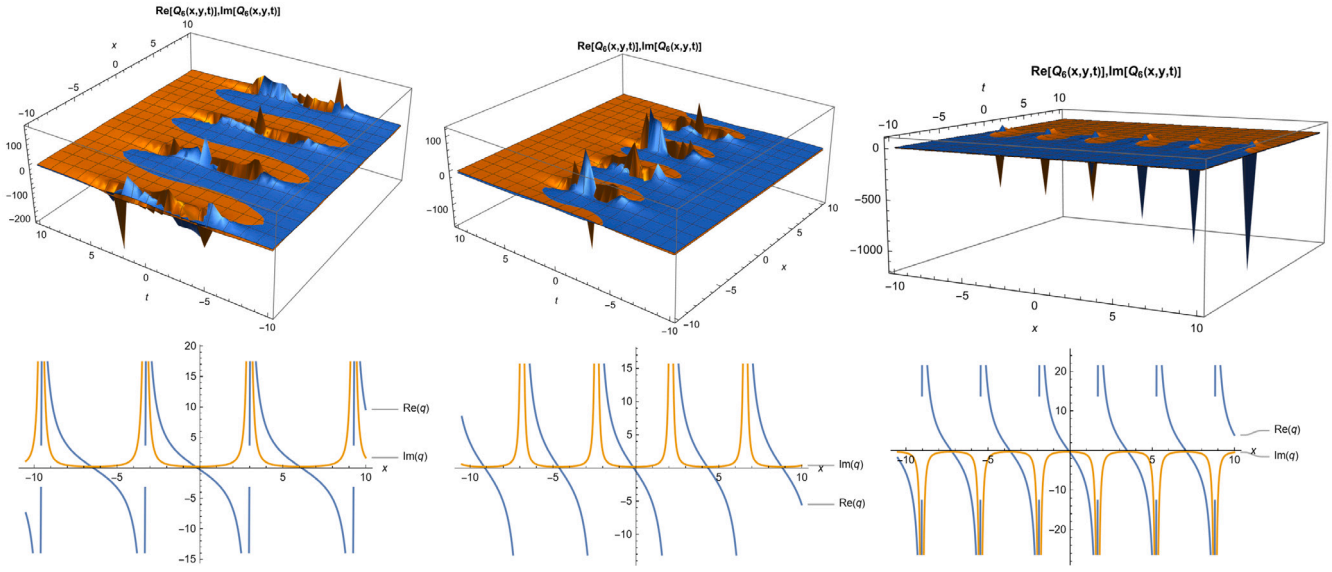


Fig. 4. The graphs of three-dimensional and two-dimensional for Eq. (5.9) at $\alpha = 0.8, l_1 = l_2 = 0.6, m_2 = 0.5, r_2 = 0.3, n_1 = 1.6, n_2 = 1.7, n_3 = 0.5$ when $m_1 = 0.5, m_1 = 0.7$ and $m_1 = 0.88$ respectively.

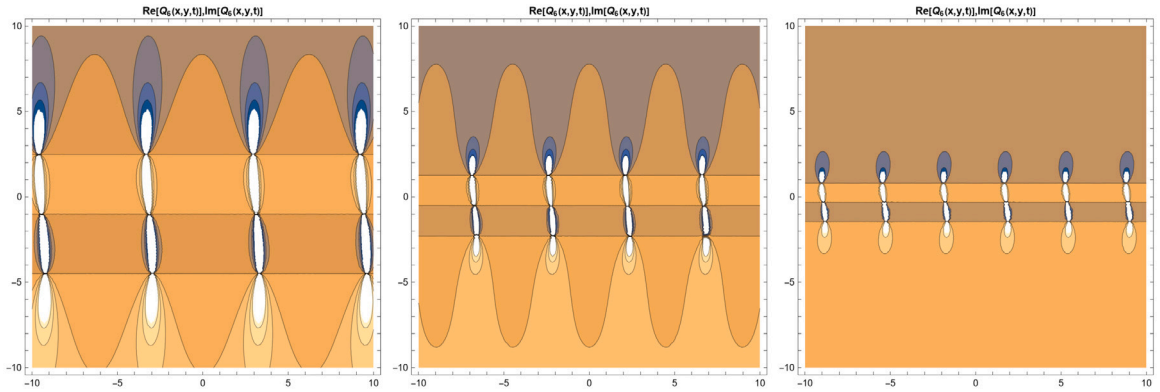


Fig. 5. The contour plots of Fig. 4 for $\alpha = 0.8, l_1 = l_2 = 0.6, m_2 = 0.5, r_2 = 0.3, n_1 = 1.6, n_2 = 1.7, n_3 = 0.5$ at $m_1 = 0.5, m_1 = 0.7$ and $m_1 = 0.88$ respectively.

by using the Eqs. (3.2), (5.1), (5.2) and (5.8), we obtain

$$Q_6(x,y,t) = -\frac{6m_1\begin{pmatrix} in_3\sinh\left(4l_2m_1^2t + l_2y - im_1x\right) + n_1\sin\left(m_1x - ir_2\left(4m_1^2t + y\right)\right) \\ +n_2\sin\left(m_2\left(4m_1^2t + y\right) + m_1x\right)\end{pmatrix}}{\alpha\begin{pmatrix} n_3\cos\left(m_1x + il_2\left(4m_1^2t + y\right)\right) + n_1\cos\left(m_1x - ir_2\left(4m_1^2t + y\right)\right) \\ +n_2\cos\left(m_2\left(4m_1^2t + y\right) + m_1x\right)\end{pmatrix}}. \tag{5.9}$$

The solution of $Q_6(x,y,t)$ is shown in three, two dimensions, and contour in Figs. 4 and 5, which show a periodic structure with well-separated lumps that follow a regular pattern. The solution has a spatial distribution of high and low values and oscillates with a specific frequency and amplitude. The lump-periodic solution behaves more steadily and is less oscillatory at lower frequency $m_1 = 0.5$. The wave retains a coherent structure with mild periodic modulation, indicating that the energy is well-localized, as indicated by the moderate periodic structure. Increasing the frequency variable to $m_1 = 0.88$ results in obtaining multi dark lump solutions which oscillate more sharply and quickly. The contour plots, show a very dense distribution of lumps with high-value regions becoming prominent, and the 3D and 2D plots exhibit this tendency. The wave patterns exhibit sharper transitions and more noticeable valleys at higher frequencies. Applications needing coherence and stability of wave structures with periodic behavior will find these insights invaluable.

Set IV:

$$r_1 = l_1,\ r_3 = -4l_1^2r_2,\ n_2 = 0,\ l_3 = -4l_1^2l_2. \tag{5.10}$$

We get

$$Q_7(x,y,t) = \frac{6l_1\left(n_1\sinh\left(r_2\left(y - 4l_1^2t\right) + l_1x\right) + n_3\sinh\left(l_2\left(y - 4l_1^2t\right) + l_1x\right)\right)}{\alpha\left(n_1\cosh\left(r_2\left(y - 4l_1^2t\right) + l_1x\right) + n_3\cosh\left(l_2\left(y - 4l_1^2t\right) + l_1x\right)\right)}. \tag{5.11}$$

One may observe how the dynamics of the generated solution Eq. (5.11) vary with frequency by looking at the surface in three-dimensional plots for various values of l_1. The solution is quite stable and shows slight slopes at $l_1 = 0.09$. The adjustments happen gradually and deliberately. A dark soliton solution, which indicates increased complexity and notable changes, is generated when the system starts to fluctuate dynamically at $l_1 = 0.5$. The system exhibits complicated and unexpected behavior as the frequency increases, going from a single dark soliton solution to an multi dark lump solution since the system gets more sensitive and unstable as the energy spreads farther.

Set V:

$$r_1 = -im_1,\ r_3 = 4m_1^2r_2,\ n_3 = 0,\ m_3 = 4m_1^2m_2. \tag{5.12}$$

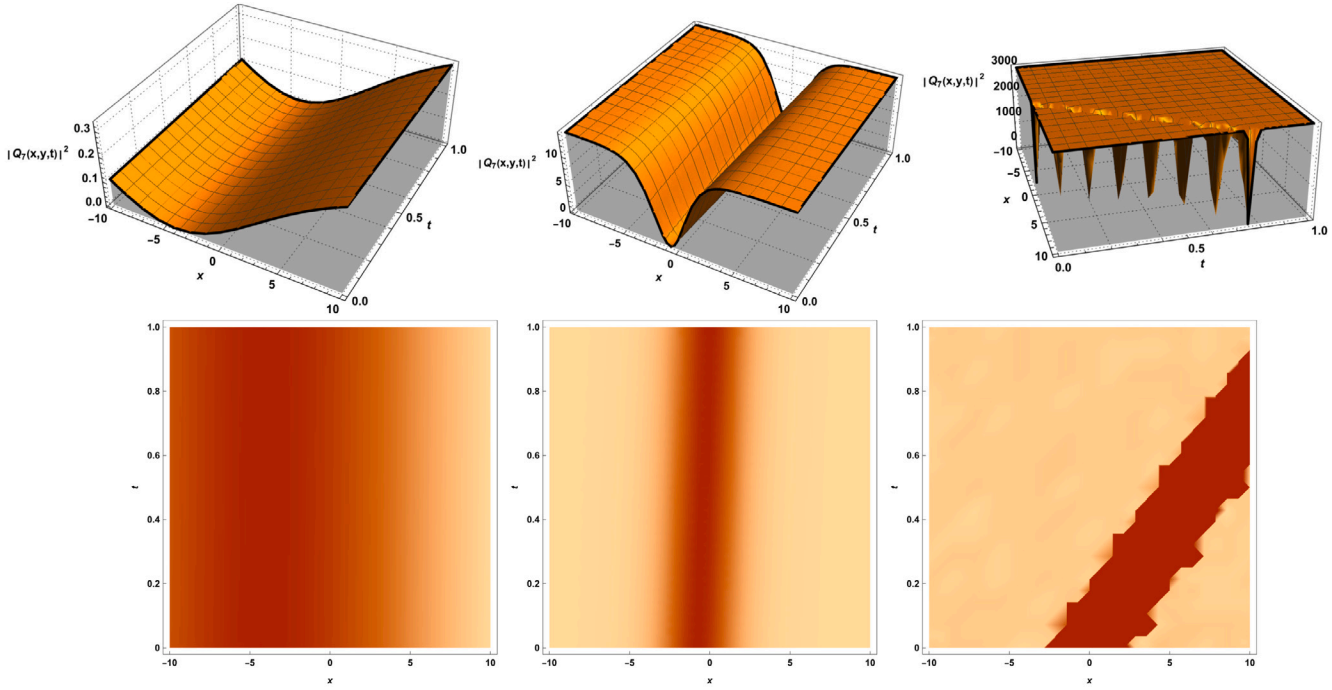


Fig. 6. The 3D and density plots of Eq. (5.11) for $\alpha = 0.8, l_2 = 0.6, r_2 = 0.3, n_1 = 1.6, n_3 = 0.5$ at $l_1 = 0.09, l_1 = 0.5$ and $l_1 = 7.5$ respectively.

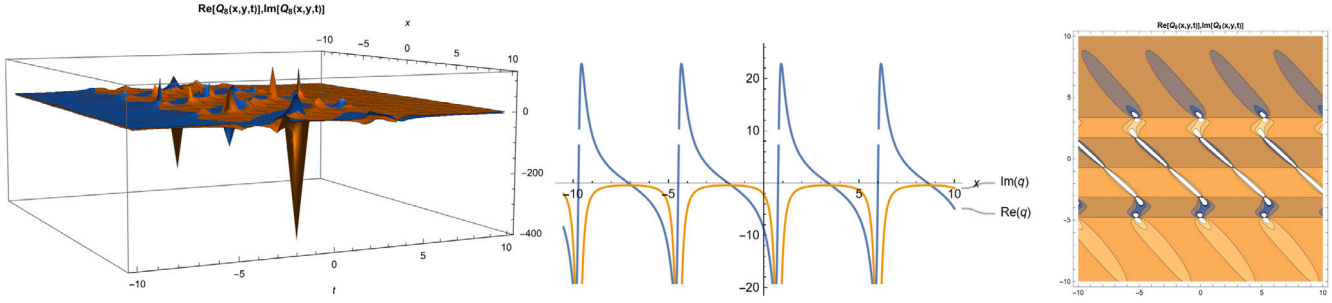


Fig. 7. The three-dimensional, two-dimensional and contour plots of Eq. (5.13) for $\alpha = 0.8, m_1 = m_2 = 0.6, r_2 = 0.3, n_2 = 1.6, n_1 = 0.5$ respectively.

We obtain

$$Q_8(x,y,t) = -\frac{6m_1\left(n_2\sin\left(m_2\left(4m_1^2t+y\right)+m_1x\right)+n_1\sin\left(m_1x+ir_2\left(4m_1^2t+y\right)\right)\right)}{\alpha\left(n_2\cos\left(m_2\left(4m_1^2t+y\right)+m_1x\right)+n_1\cos\left(m_1x+ir_2\left(4m_1^2t+y\right)\right)\right)}. \tag{5.13}$$

The real component of Eq. (5.13) is shown in a $3D$ graphic, which shows localized wave patterns as peaks and troughs throughout a range of x and y values. This makes spatial behavior, such wave propagation or energy distribution, easier to understand. Using contour lines to represent different values, a contour plot provides a top-down view of the values of the function. Contour plots are commonly used to illustrate potential fields, such as electric or gravitational fields, where lines indicate areas of equal potential. A $2D$ figure shows the cross-sections of the function's real and imaginary components along certain axes illustrates oscillatory activity and the relationship between the real and imaginary components. It is necessary to understand how a function evolves across time or space.

6. The two-wave solutions

Let us assume that the function g has the following structure so that we can obtain the precise two-wave solution in this section

$$g(x,y,t) = e^{\mu_1}n_1 + e^{-\mu_1}n_2 + n_3\sin\left(\mu_2\right) + n_4\sinh\left(\mu_3\right), \tag{6.1}$$

where

$$\begin{aligned}\mu_1 &= m_2t + m_1y + x,\\ \mu_2 &= m_4t + m_3y + x,\\ \mu_3 &= m_6t + m_5y + x.\end{aligned} \tag{6.2}$$

where m_1, m_2, m_3, m_4, m_5 and m_6 are constants, we get The following when the above relations are used.

$$\begin{aligned}16m_1n_1n_2 + 4m_2n_1n_2 &= 0,\\ -2m_1n_1n_3 - m_2n_1n_3 + 2m_3n_1n_3 - m_4n_1n_3 &= 0,\\ -2m_1n_1n_3 + m_2n_1n_3 - 2m_3n_1n_3 - m_4n_1n_3 &= 0,\\ 2m_1n_2n_3 + m_2n_2n_3 - 2m_3n_2n_3 + m_4n_2n_3 &= 0,\\ -2m_1n_2n_3 + m_2n_2n_3 - 2m_3n_2n_3 - m_4n_2n_3 &= 0,\\ 4m_3n_3^2 - m_4n_3^2 &= 0,\\ -4m_1n_1n_4 - m_2n_1n_4 - 4m_5n_1n_4 - m_6n_1n_4 &= 0,\\ 4m_1n_1n_4 + m_2n_1n_4 + 4m_5n_1n_4 + m_6n_1n_4 &= 0,\\ 4m_1n_2n_4 + m_2n_2n_4 + 4m_5n_2n_4 + m_6n_2n_4 &= 0,\\ 4m_1n_2n_4 + m_2n_2n_4 + 4m_5n_2n_4 + m_6n_2n_4 &= 0,\\ 2m_3n_3n_4 - m_4n_3n_4 - 2m_5n_3n_4 - m_6n_3n_4 &= 0,\\ -2m_3n_3n_4 - m_4n_3n_4 - 2m_5n_3n_4 + m_6n_3n_4 &= 0,\end{aligned} \tag{6.3}$$

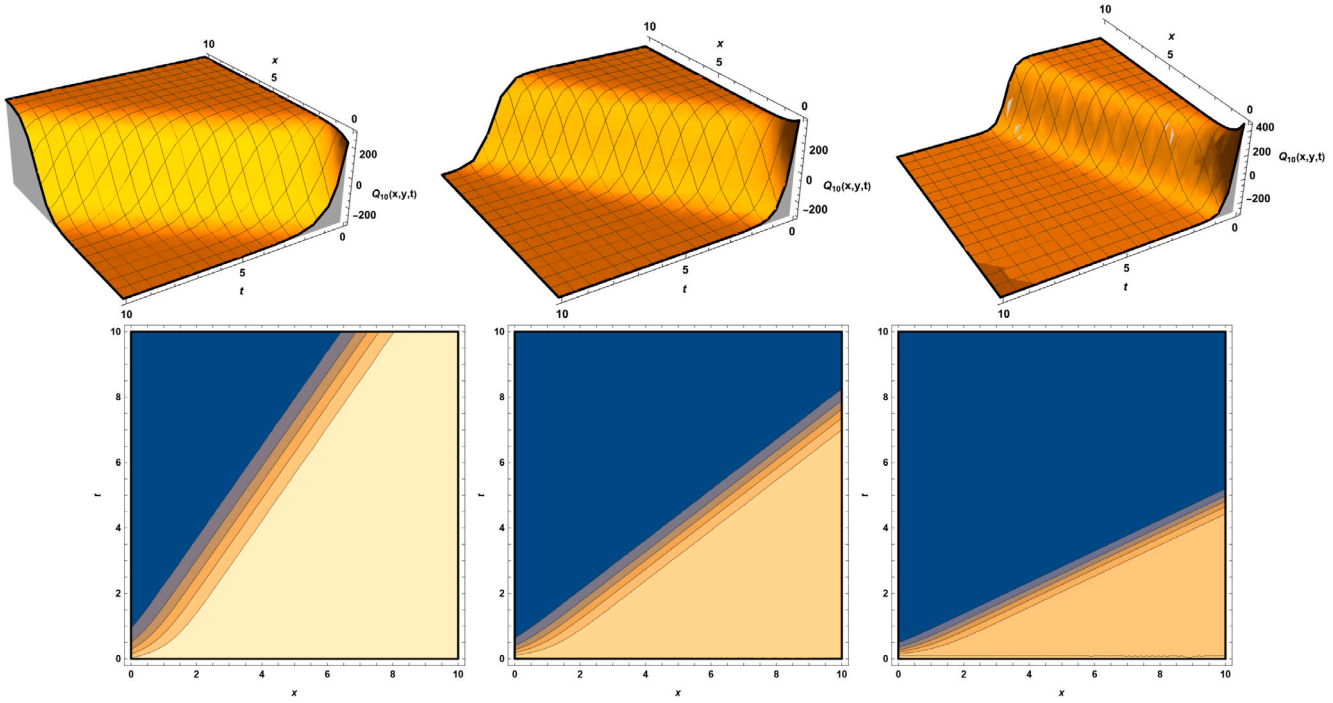


Fig. 8. The three-dimensional and contour plots of Eq. (6.7) using $\alpha = 0.02, m_6 = 0.6, n_1 = 0.2, n_2 = 0.9, n_4 = 0.8$ at $m_1 = 0.5, m_1 = 0.8$ and $m_1 = 1.2$ respectively.

$$-4m_5n_4^2 - m_6n_4^2 = 0, 4m_5n_4^2 + m_6n_4^2 = 0.$$

We obtain the following sets of solutions by using Eqs. (6.1), (3.3) and (6.2):

Set I: When

$$m_2 = -4m_1,\ m_5 = -\frac{m_6}{4},\ n_2 = 0; n_3 = 0. \tag{6.4}$$

The two-wave solution of Eq. (3.1) is obtained by using these values

$$Q_9(x,y,t) = \frac{6\left(n_4 e^{4m_1 t}\cosh\left(m_6\left(t-\frac{y}{4}\right)+x\right)+n_1 e^{m_1 y+x}\right)}{\alpha\left(n_4 e^{4m_1 t}\sinh\left(m_6\left(t-\frac{y}{4}\right)+x\right)+n_1 e^{m_1 y+x}\right)}. \tag{6.5}$$

Set II:

$$m_2 = -4m_1,\ m_5 = -\frac{m_6}{4},\ n_3 = 0. \tag{6.6}$$

These values give

$$Q_{10}(x,y,t) = \frac{6\left(n_4 e^{m_1(4t+y)+x}\cosh\left(m_6\left(t-\frac{y}{4}\right)+x\right)-n_2 e^{8m_1 t}+n_1 e^{2(m_1 y+x)}\right)}{\alpha\left(n_4 e^{m_1(4t+y)+x}\sinh\left(m_6\left(t-\frac{y}{4}\right)+x\right)+n_2 e^{8m_1 t}+n_1 e^{2(m_1 y+x)}\right)}. \tag{6.7}$$

Set III:

$$m_6 = -4m_5,\ n_1 = 0,\ n_2 = 0,\ n_3 = 0. \tag{6.8}$$

The following solution is retrieved

$$Q_{11}(x,y,t) = \frac{6\coth\left(m_5(y-4t)+x\right)}{\alpha}. \tag{6.9}$$

7. Results and discussions

In this work, the lump interaction principles of an acoustic wave equation in harmonic crystals are investigated using the Hirota bilinear approach. It has been demonstrated that lump wave solutions are among the most effective ones for non-linear evolution equations. The successful reporting of several lump-wave, two-wave, and lump-periodic wave solutions. In physics, maths, and related fields, a wave is an expanding dynamic disturbance of one or more parameters. When a wave is periodic, its components oscillate regularly at a certain frequency in the vicinity of an equilibrium value. A standing wave, in comparison, is made up of two superimposed periodic waves that travel in the opposing directions. A wave is said to be a traveling wave if the entire waveform is moving in the same direction. The vibrational amplitude of the standing waves in certain places has nulls where the wave phase seems to be 0 or very low.[47]

When the parameters are set to have good values, plots in three-dimensions, two-dimensions, density, and contour are presented. These plots are used to examine the evolutionary traits of wave solutions and study their dynamics. Figs. 1 and 2 illustrate the evolution and dynamical characteristics of the lump wave solutions obtained using the suitable parameters given above. Figs. 1 and 2 depict the solution in three dimensions, two dimensions and density pictures of Eq. (4.5). The three-dimensional graphic in the complete view is where we discover the periodic qualities. The density, contour, three-dimensional and two-dimensional images in Figs. 1 and 2 are obtained by extending the range to widen the observation waveform. The lump waves, which travel in the x-axis's positive direction and experience periodic alterations, are what we can observe. Figs. 3–7 show the collision characteristics between the exponential function, lump wave and singular periodic wave for the lump–periodic wave solutions. We can observe the two lump waves, one with a crest higher than the water and one with a dip lower than the water together with some periodic waves in Fig. 3, as l_1 increases the lump-periodic waves increase and move diagonally. As seen in Fig. 4, when the velocity of the wave m_1 is increased, the peak of the lump wave steadily decreases which results in the restoration of the 6 dark soliton solutions which are known to be dark-lump wave solutions, their corresponding contour graphs are displayed in Fig. 5. Interesting graphs can be observed from the simulation of Eq. (5.11), when the graph of $\left|Q_7(x,y,t)\right|^2$ is constructed, the kink soliton solution is obtained, as the velocity of the wave l_1 is increased the dark soliton and 8-dark lump wave solutions are generated. The 3-dark lump waves together with some periodic waves can be seen in Fig. 7. Figs. 8 and 9 show the collision characteristics between the singular periodic, exponential function and lump waves for the two-wave solutions.

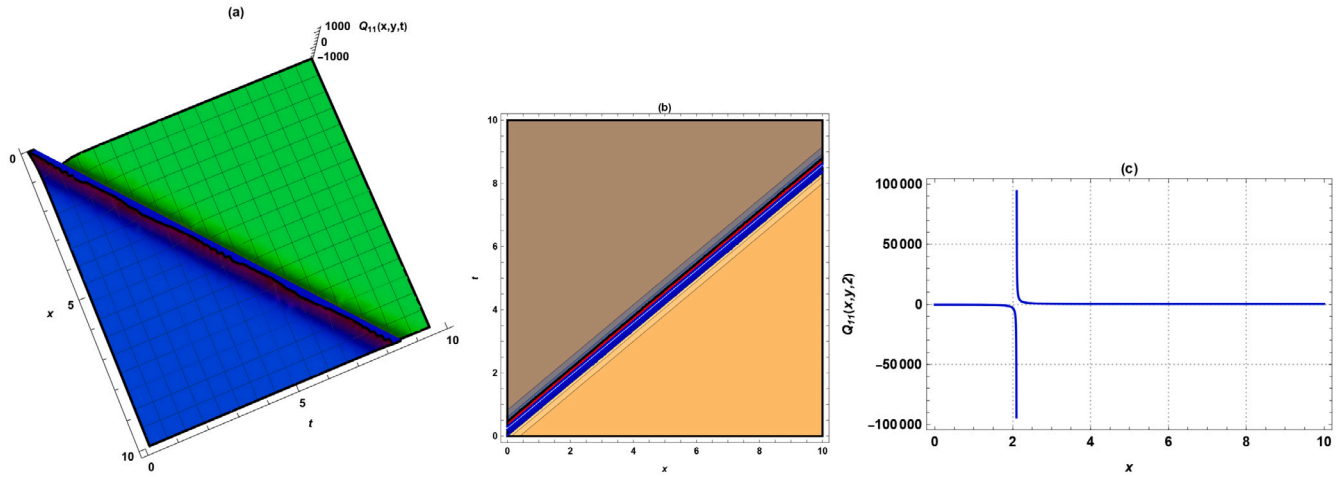


Fig. 9. The three-dimensional, contour and two-dimensional plots of Eq. (6.9) for $\alpha = 0.02, m_5 = 0.3$ respectively.

If the real symmetric matrix $A = (a_{ij})_{M\times M}$ is positive definite in the quadratic function g as defined by Ma et al.[48], then $g \to \infty$ when $|x| \to \infty$ in any direction within R^N, which ensures that $Q(x, y, t) = \frac{6}{\alpha}(\ln g)_x \to 0$ as $|x| \to \infty$ in any direction in R^N, and results in the formation of lump solutions, rationally localized solutions in both space and time directions. On the other hand, if A is positive semidefinite, then $Q(x, y, t) = \frac{6}{\alpha}(\ln g)_x$ does not go to zero in other word vanish in all directions in R^N but may go to zero in all directions in a subspace of R^N. As a result, lump-type solutions are usually the end outcome in these situations. Fortunately, the solutions obtained are, in fact, lump solutions if the appropriate subspace corresponds to the entire space to which the spatial variables belong.[48]

8. Conclusion

The new KdV model has significantly advanced our understanding of a number of physical phenomena, such as ion-acoustic waves in plasma and acoustic waves in harmonic crystals. With the help of Hirota linearization and the proper transformation, the new KdV equation is solved analytically. The generated solutions contain many solitary wave types, including lump waves in the form of lump-periodic wave solutions, two-wave solutions, and lump waves in the form of dark-bright lump wave solutions. The results have important ramifications for a number of intriguing scientific phenomena, such as ion-acoustic waves in plasma, acoustic waves in harmonic crystals, and shallow-water waves. The investigation's findings might assist to create new scientific applications. Based on the choice of suitable parameter values, numerical simulations of the reported results are provided. New information and ideas about the innovative $(2 + 1)-$dimensional KdV equation were undoubtedly offered by the study's findings.

We conclude with the expectation that our results will be a starting point for further studies of the lump solutions and their impact on the evolving behavior of nonlinear wave occurrences. By doing so, we contribute to the broader area of mathematical techniques, deepen our understanding of complicated nonlinear dynamics, and pave the way for innovative applications in a range of scientific domains. Acoustic waves in harmonic crystals, ion-acoustic waves in plasma, including shallow-water waves, and other fascinating scientific phenomena all benefit from the discovery. In future we aim to find the lump solution of the higher dimensional KdV and PDEs in general.

CRediT authorship contribution statement

Muhammad Abubakar Isah: Conceptualization, Methodology, Software, Data curation, Writing – original draft, Visualization, Investigation. **Asif Yokus:** Supervision, Software, Validation, Writing – review & editing. **Ibrahim Isah:** Supervision, Writing – review & editing.

Declaration of competing interest

The authors declare that they have no known competing financial interests or personal relationships that could have appeared to influence the work reported in this paper.

Acknowledgments

All authors discussed the results and contributed to the final manuscript

Data availability

No data was used for the research described in the article.

References

1. Duran S, Doğan K. Breaking analysis of solitary waves for the shallow water wave system in fluid dynamics. *Eur Phys J Plus*. 2021;136(9):1–12.
2. Isah MA, Isah I, Hassan TL, Usman M. Some characterization of osculating curves according to darboux frame in three dimensional euclidean space. *J Adv Acad Res*. 2021;7(12):47–56. 2021.
3. Isah I, Isah MA, Baba MU, Hassan TL, Kabir KD. On integrability of silver Riemannian structure. *J Adv Acad Res*. 2021;7(12):2488–9849.
4. Isah MA, Külahcı MA. A study on null cartan curve in Minkowski 3-space. *Appl Math Nonlinear Sci*. 2020;5(1):413–424.
5. Isah MA, Külahcı MA. Special curves according to bishop frame in Minkowski 3-space. *Appl Math Nonlinear Sci*. 2020;5(1):237–248.
6. Isah MA, Külahcı MA. Involute curves in 4-dimensional Galilean space G4. In: *CPOST*. 2019:134–141. Vol. 2, (2).
7. Myint-U T, Debnath L. *Linear Partial Differential Equations for Scientists and Engineers*. Spr Sci Biz Media; 2007.
8. Scott Ac, Chu FYF, McLaughlin DW. The soliton: a new concept in applied science. *Proc IEEE*. 1973;61(10):1443–1483.
9. Isah MA, Yokus A, Kaya D. Exploring the influence of layer and neuron configurations on Boussinesq equation solutions via a bilinear neural network framework. *Nonlinear Dynam*. 2024;112(15):13361–13377.
10. Yokus A, Isah MA. Stability analysis and solutions of (2+ 1)-Kadomtsev–Petviashvili equation by homoclinic technique based on Hirota bilinear form. *Nonlinear Dynam*. 2022;109:3029–3040.
11. Kumar A, Arora R. Soliton solution for the BBM and MRLW equations by cosine-function method. *Adv Mod Opt Comput*. 2011.

12. Duran S, Yokuş A, Durur H. Surface wave behavior and refraction simulation on the ocean for the fractional Ostrovsky–Benjamin–Bona–Mahony equation. *Mod Phys Lett B*. 2021;35(31):2150477.
13. Duran S, Karabulut B. Nematicons in liquid crystals with Kerr law by sub-equation method. *Alex Eng J*. 2022;61(2):1695–1700.
14. Duran S, Yokus A, Kaya D. Evolution dynamics of fundamental mechanisms of wave propagation in gas bubble-liquid interactions and soliton solutions. *Phys Scr*. 2025;100(2):025229.
15. Zhang RF, Bilige S. Bilinear neural network method to obtain the exact analytical solutions of nonlinear partial differential equations and its application to p-gBKP equation. *Nonlinear Dynam*. 2019;95:3041–3048. http://dx.doi.org/10.1007/s11071-018-04739-z.
16. Isah MA, Yokus A, Kaya D. Bilinear neural network method for obtaining the exact analytical solutions to nonlinear evolution equations and its application to KdV equation. *Khayyam J Math*. 2024;10(2):228–248.
17. İskenderoğlu G, Kaya D. Lie symmetry analysis of Caputo time-fractional k (m, n) model equations with variable coefficients. *Sigma J Eng Nat Sci*. 2024;42(3):885–889.
18. Duran S, Kaya D. Applications of the sub equation method for the high dimensional nonlinear evolution equation. *Erzincan Univ J Sci Technol*. 2021;14(3):898–906.
19. Zhang RF, Li MC. Bilinear residual network method for solving the exactly explicit solutions of nonlinear evolution equations. *Nonlinear Dynam*. 2022;108(1):521–531.
20. Akbulut A, Sajjad HM, Rezazadeh H. New conservation laws and exact solutions of coupled Burgers' equation. *Waves Random Complex Media*. 2021:1–20.
21. Duran S. Breaking theory of solitary waves for the Riemann wave equation in fluid dynamics. *Int J Mod Phys B*. 2021;35(09):2150130.
22. Durur H. Energy-carrying wave simulation of the Lonngren-wave equation in semiconductor materials. *Int J Mod Phys B*. 2021;35(21):2150213.
23. Debin K, Rezazadeh H, Ullah N, Vahidi J, Tariq KU, Akinyemi L. New soliton wave solutions of a (2+ 1)-dimensional Sawada–Kotera equation. *J Ocean Eng Sci*. 2023;8(5):527–532.
24. Kaya D, Yokuş A, Demiroğlu U. Comparison of exact and numerical solutions for the Sharma–Tasso–Olver equation. In: *Numerical Solutions of Realistic Nonlinear Phenomena*. Cham: Springer; 2020:53–65. Vol. 31.
25. Zekavatmand SM, Rezazadeh H, Inc M, Vahidi J, Ghaemi MB. The new soliton solutions for long and short-wave interaction system. *J Ocean Eng Sci*. 2022;7(5):485–491.
26. Darwish A, Ahmed HM, Ammar M, Ali MH, Arnous AH. General solitons and other solutions for coupled system of nonlinear Schrödinger's equation in magneto-optic waveguides with anti-cubic law nonlinearity by using improved modified extended tanh-function method. *Opt*. 2022;251:168369.
27. Akram G, Sadaf M, Khan MAU. Abundant optical solitons for Lakshmanan–Porsezian–Daniel model by the modified auxiliary equation method. *Opt*. 2022;251:168163.
28. Yokus A, Isah MA. Investigation of internal dynamics of soliton with the help of traveling wave soliton solution of Hamilton amplitude equation. *Opt Quantum Electron*. 2022;54:528.
29. Isah MA, Yokuş A. The investigation of several soliton solutions to the complex Ginzburg–Landau model with Kerr law nonlinearity. *Math Model Numer Simul Appl*. 2022;2(3):147–163.
30. Isah MA, Yokus A. The novel optical solitons with complex Ginzburg–Landau equation for parabolic nonlinear form using the Q6-model expansion approach. *MESA J Math Eng Sci Aerosp*. 2023;14(1):205–225.
31. Isah MA, Yokus A. A novel technique to construct exact solutions for the complex Ginzburg–Landau equation using quadratic-cubic nonlinearity law. *J| MESA J Math Eng Sci Aerosp*. 2023;14(1):239–260.
32. Isah MA, Yokus A. Application of the newly φ^6-model expansion approach to the nonlinear reaction–diffusion equation. *Open J Math Sci*. 2022;6(1):269–280.
33. Yokus A, Isah MA. Unveiling novel insights: Nonlinear dispersion dynamics of optical solitons through new φ^6-model expansion in the Klein–Gordon equation. *Chinese J Phys*. 2025;95:476–492.
34. Seadawy AR, Ahmed S, Rizvi STR, K. Ali. Lumps, breathers, interactions and rogue wave solutions for a stochastic gene evolution in double chain deoxyribonucleic acid system. *Chaos Solitons Fractals*. 2022;161:112307.
35. Ahmed S, Ashraf R, Seadawy AR, Rizvi STR, Younis M, Althobaiti A, El-Shehawi AM. Lump multi-wave kinky breathers interactional solutions and stability analysis for general (2+1)-rth dispersionless dym equation. *Results Phys*. 2021;25:104160.
36. Yusuf A, Sulaiman TA. Dynamics of lump-periodic breather and two-wave solutions with the long wave in shallow water under gravity and 2D nonlinear lattice. *Commun Nonlinear Sci Num Simul*. 2021;99:105846.
37. Ma WX. A search for lump solutions to a combined fourth order nonlinear PDE in $(2+1)-$dimensions. *J Appl Anal Comput*. 2019;9:1319–1332.
38. Sulaiman TA, Yusuf A, Atangana A. New lump, lump-kink, breather waves and other interaction solutions to the (3+1)dimensional soliton equation. *Commun Theor Phys (Beijing)*. 2020;72:085004.
39. Sulaiman TA, Yusuf A, Alshomrani AS, Baleanu D. Lump collision phenomena to a nonlinear physical model in coastal engineering. *Math*. 2022;10(15):2805.
40. Arif MG, Islam Z, Begum M, Sheikh MAN. Dynamical behaviors of a new KdV model via Hirota's bilinear formulation. *Partial Differ Equ Appl Math*. 2022;6:100410.
41. Hietarinta J. A search for bilinear equations passing Hirota's three-soliton condition. I. KdV-type bilinear equations. *J Math Phys*. 1987;28(8):1732–1742.
42. Ghanbari B. Employing hirota's bilinear form to find novel lump waves solutions to an important nonlinear model in fluid mechanics. *Results Phys*. 2021;29:104689.
43. Griffiths GW. *Hirota Direct Method*. City Uni London.; 2012.
44. Wang CJ, Dai ZD, Mu G, Li SQ. New exact periodic solitary-wave solutions for new (2+ 1)-dimensional KdV equation. *Commun Theor Phys*. 2009;52(5):862.
45. Shen S. Lie symmetry analysis and Painlevé analysis of the new (2+1)-dimensional KdV equation. *Appl Math Chin Univ*. 2007;22:207–212. http://dx.doi.org/10.1007/s11766-007-0209-2.
46. Zhang YF, Tam H, Zhao J. Higher-dimensional KdV equations and their solitonsolutions. *Commun Theor Phys*. 2006;45(3):411.
47. Chakravorty P. What is a signal? lecture note. *IEEE Signal Process Mag*. 1982;35(5):175–177.
48. Ma WX, Zhou Y. Lump solutions to nonlinear partial differential equations via Hirota bilinear forms. *J Differential Equations*. 2018;264(4):2633–2659.